

1 **RESPONSES TO EDITOR:**

2 Thank you very much for all your suggestions and comments. Next, we respond all your questions  
3 in order:

4 1. All three reviewers question the selection of the GEV distribution and call for additional  
5 statistical metrics to justify this decision. The authors may wish to consider the use of relative  
6 quality estimators as additional statistical metrics to compare the different distribution models  
7 and corroborate the current results.

8 Answer: The quality estimator is the percentage of intervals that pass the  $\chi^2$  test for every PDF  
9 candidate. For example: if we use  $\chi^2$  test with 10 classes we obtain: GEV 41.2%, Beta 29.4%,  
10 Normal 23.5% and Gamma 17.6%. Therefore the best is GEV.

11 We have added the following clarifications.

12 Page 20, line 557 (in this document):

13 “The statistical metric used in this study to assess the fit of the observed NDVI values with  
14 respect to the PDF candidates (Normal, Gamma, Beta and GEV) was the Chi square test ( $\chi^2$  test).  
15 The following steps were carried out:

16

17 1. MLM was applied to model these 46 RV. Parameters were calculated for the four PDF  
18 candidates (see Table 2).

19 2. To check the goodness of the fit of PDF candidates, Chi square test ( $\chi^2$  test) was applied  
20 from 7 classes to 14 classes meeting the requirement that each class has at least five  
21 observations. The level of significance ( $\alpha$ ) was fixed to 5% for all the candidates.”

22

23 Page 21, line 599:

24 “Twelve intervals (from 23 to 34) corresponding to months of July, August and September  
25 have been excluded of this analysis since these intervals fall into the dry season in the study area,  
26 normally not cover by any SIBI. Therefore, calculations were carried out over 34 intervals.

27

28 To assess the general goodness of fit, the number of intervals where the  $\chi^2$  test was accepted (or  
29 failed to reject) was calculated for every PDF candidate. Then, the percentage of accepted  
30 intervals, over the total 34 intervals, was also calculated (the quality estimator). Fig. 8 shows this  
31 percentage of intervals that fit for every PDF candidate. The number of classes used in  $\chi^2$  test is  
32 represented at X-axis (from 7 to 14 classes).”

33 Our procedure has been to explore if a PDF could be used for a set of data respect to an interval.  
34 Sometimes all the PDF candidates could be used because all of them passed the  $\chi^2$  test, other  
35 times only some of them. The best PDF candidate to be used along the year is the one with the  
36 highest percentage of intervals that passed the  $\chi^2$  test (quality estimator). We are open to other

37 quality estimator that the editor suggests. In any case, the aim of this study is not to prove that  
38 GEV is the best possible fit, but to prove there are PDF candidates better than Normal.

39

40 2. Reviewer 3 calls for a literature review in the introduction (with additional references) on NDVI  
41 distribution functions and limitations to the use of the normal distribution. Unfortunately these  
42 issues have not been addressed in the interactive comments, but will definitely help the  
43 formulation of discussion points.

44 We have added the following clarifications and references.

45 Page 7, line 213:

46 “Important NDVI-based indices of detecting drought are NDVI anomalies (NDVIA) and  
47 Standardized Vegetation Index (SVI). NDVIA and SVI have been successfully used to monitor  
48 drought conditions over different regions on the world (Nanzad et al., 2019; Li et al., 2014). NDVIA  
49 is calculated as the difference between the NDVI value for a specific time period (e.g., week,  
50 month) and the long-term mean value for that period. SVI was developed by Peters et al. (2002)  
51 and obtains the probability from normal NDVI distributions over multiple years of data, on a time  
52 period (Anyamba and Tucker, 2012; Bayarjargal et al., 2006). It is defined as:

53

$$54 \quad SVI_i = \frac{NDVI_i - \overline{NDVI}}{\sigma_{NDVI}} = \frac{NDVIA_i}{\sigma_{NDVI}} \quad (1)$$

55

56 where  $\overline{NDVI}$  is the long-term mean NDVI in the period  $i$ ,  $\sigma_{NDVI}$  is the standard deviation of NDVI  
57 in the period  $i$ , and  $NDVI_i$  is the current NDVI value in the time period  $i$ . Using only the first and  
58 second statistical moment, average and the square root of variance, assumption of normality is  
59 implicit in this type of drought NDVI indicator.”

60 If there are other references that we should include we will appreciate that you point out.

61

62 3. The manuscript lacks a separate discussion section: the authors should consider a split between  
63 results and discussion. A separate dedicated section will help formulate strengths and weaknesses  
64 of the study such as temporal, spatial and spectral scales, the representativeness for a wider area  
65 and applicability to another environment. This section is necessary to place the research in a larger  
66 context and relate the findings to other research.

67 Answer: We have split between results and discussion as it can be seen in the last version of the  
68 manuscript.

69

70 4. On a more technical level, the following description may be added to address Reviewer 1's  
71 comments on atmospheric correction. "Each MOD09A1 pixel contains the best possible L2G  
72 observation during an 8-day period as selected on the basis of high observation coverage, low  
73 view angle, the absence of clouds or cloud shadow, and aerosol loading." However, certain  
74 observations were removed from further analysis, and therefore the question remains on what  
75 basis these observations were removed.

76 Answer: We have added the description.

77 Page 11, line 364:

78 "Each MOD09A1 pixel contains the best possible L2G observation during an 8-day period as  
79 selected on the basis of high observation coverage, low view angle, the absence of clouds or cloud  
80 shadow, and aerosol loading."

81

82 5. I have serious concerns with respect to the (colour) filtering technique which seems to remove  
83 all NDVI values below 0.2-0.25. This removal needs further explanation (or even exploration) in  
84 view of the proposed extreme value distributions.

85 Answer: We have clarified the HSL filtering technique.

86 Page 16, line 490:

87 "MOD09A1 is a MODIS product that processes data to obtain the best observation in an 8-  
88 days period. However, it is possible that the result of this selection still presents some problems  
89 since the best of this selection is relative to the eight observations of the period. For example, if  
90 the eight observations, at one pixel, appear with clouds, shadow clouds or snow, the best  
91 selection still maintains this problem.

92

93 As an example of above, the NDVI series (10 years) of one pixel of the study area is shown in  
94 Fig. 3. On the top graph of Fig. 3 it is noticed that there exit some extremely low NDVI values in  
95 some dates. If these NDVI values are compared to neighbor values (8 days after or before) the high  
96 variation presented in such short period is not believable. This issue tells us that MODIS sensor has  
97 not obtained a proper observation in this 8 days period (interval).

98

99 HSL criterion helps us to eliminate these incorrect NDVI values, since the filter is interpreting  
100 that these pixels still contains clouds or snow, i.e., pixels with low saturation (greyish colours)."

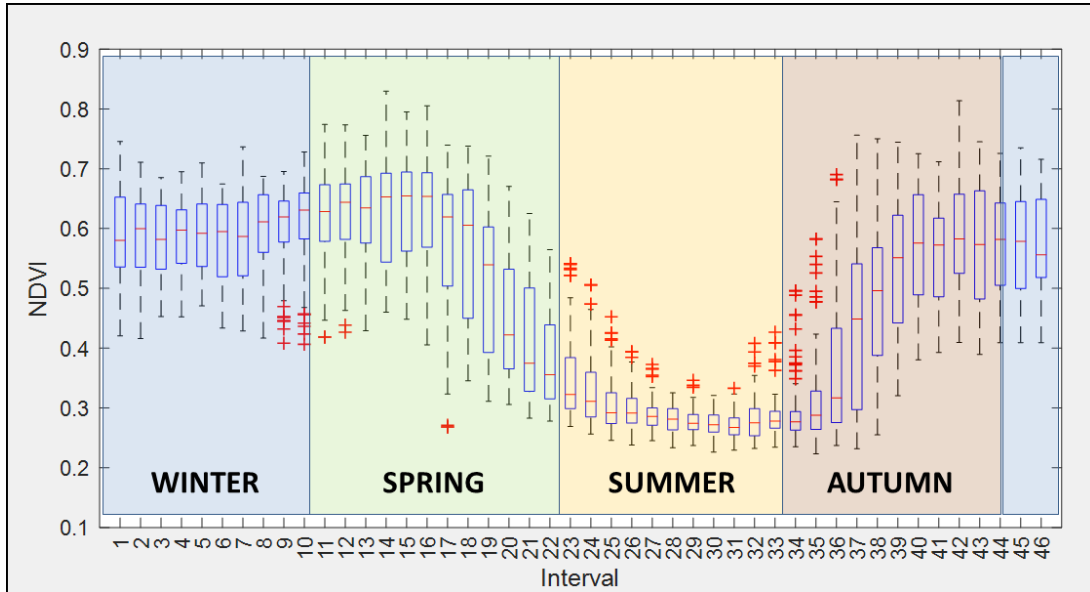
101

102 6. The mean NDVI profile presented in Figure 4 is very informative. However, an indication of  
103 inter-quartile range would be even more informative, for instance in the form of a box plot. The  
104 characterization of this seasonal variation and its explanation in agronomic terms seems crucial for

105 the general understanding of the manuscript. The authors have the data to undertake this  
106 analysis.

107 Answer: We have added boxplots in Figure 4.

108 Page 19:



109

110 **Figure 4.** Box plots of 46 random variables (RV) are shown as well as start and end reference of  
111 every season. Study period from 2002 to 2017.

112

113

# Statistical Analysis for Satellite Index-Based Insurance to define Damaged Pasture Thresholds

Juan José Martín-Sotoca<sup>1\*</sup>, Antonio Saa-Requejo<sup>2,3</sup>, Rubén Moratíel<sup>2,3</sup>, Nicolas Dalezios<sup>4</sup>, Ioannis Faraslis<sup>5</sup>, and Ana María Tarquis<sup>2,6</sup>

jmartinsotoca@gmail.com, antonio.saa@upm.es, ruben.moratíel@upm.es, dalezios.n.r@gmail.com, faraslisgiannis@yahoo.gr, anamaria.tarquis@upm.es

<sup>1</sup> Data Science Laboratory. European University, Madrid, Spain.

<sup>2</sup> CEIGRAM, Research Centre for the Management of Agricultural and Environmental Risks, Madrid, Spain.

<sup>3</sup> Dpto. Producción Agraria. Universidad Politécnica de Madrid, Spain.

<sup>4</sup> Department of Civil Engineering. University of Thessaly, Volos, Greece.

<sup>5</sup> Department of Planning and Regional Development. University of Thessaly, Volos, Greece.

<sup>6</sup> Grupo de Sistemas Complejos. Universidad Politécnica de Madrid, Spain.

\* Correspondence to: jmartinsotoca@gmail.com

**Abstract:** Vegetation indices based on satellite images, such as Normalized Difference Vegetation Index (NDVI), have been used in countries like USA, Canada and Spain for damaged pasture and forage insurance for the last years. This type of agricultural insurance is called “satellite index-based insurance” (SIBI). In SIBI, the occurrence of damage is defined through NDVI thresholds mainly based on statistics derived from Normal distributions. In this work a pasture area at the north of Community of Madrid (Spain) has been delimited by means of Moderate Resolution Imaging Spectroradiometer (MODIS) images. **A statistical analysis of NDVI histograms was applied to seek for alternative distributions using maximum likelihood method and  $\chi^2$  test.** The results show that the Normal distribution is not the optimal representation and the General Extreme Value (GEV) distribution presents a better fit through the year **based on a quality estimator.** A comparison between Normal and GEV are showed respect to the probability under a NDVI threshold value along the year. This suggests that a priori distribution should not be selected and a percentile methodology should be used to define a NDVI damage threshold rather than the average and standard deviation, typically of Normal distributions.

**Keywords:** NDVI, pasture insurance, GEV distribution, MODIS.

---

## Highlights

- **The GEV distribution provides better fit to the NDVI historical observations than the Normal one.**
- **Difference between Normal and GEV distributions are higher during spring and autumn, transition periods in the precipitation regimen.**
- **NDVI damage threshold shows evident differences using Normal and GEV distributions covering both the same probability (24.20%).**

- **NDVI damage threshold values based on percentiles calculation is proposed as an improvement in the index based insurance in damaged pasture.**

154

## 155 **1. Introduction**

156 Agricultural insurance addresses the reduction of the risk associated with crop  
157 production and animal husbandry. The concept of index-based insurance (IBI) attempts to  
158 achieve settlements based on the value taken by an objective index rather than on a case-  
159 by-case assessment of crop or livestock losses (Gommes and Kayitakier, 2013). Indeed, the  
160 goal of IBI policy remains to develop an affordable tool to all producers, including  
161 smallholders. Specifically, IBI can constitute a safety net against weather-related risks for  
162 all members of the farming community, thereby increasing food security and reducing the  
163 vulnerability of rural populations to weather extremes. Moreover, IBI can be associated  
164 with credits for insured smallholders, due to the fact that the risk of non-repayment for  
165 lenders is reduced, which encourages the use of agricultural inputs and equipment,  
166 leading to increased and more stable crop production. Over the past decade, the  
167 importance of weather index-based insurances (WIBI) for agriculture has been increasing,  
168 mainly in developing countries (Gommes and Kayitakier, 2013). This interest can be  
169 explained by the potential that IBI constitutes a risk management instrument for small  
170 farmers. Indeed, it can be considered within the context of renewed attention to  
171 agricultural development as one of the milestones of poverty reduction and increased  
172 food security, as well as the accompanying efforts from various stakeholders to develop  
173 agricultural risk management instruments, including agricultural insurance products.

174

175 Farmers need to protect their land and crops specifically from drought in arid and  
176 semi-arid countries, since their production may directly depend mainly on the impacts of  
177 this particular natural hazard. Insurance for drought-damaged lands and crops is currently  
178 the main instrument and tool that farmers can resort in order to deal with agricultural  
179 production losses due to drought. Many of these insurances are using satellite vegetation  
180 indices (Rao, 2010), thus they are also called “satellite index-based insurances” (SIBI). SIBI  
181 have some advantages over WIBI, such as cost-effective information and acceptable  
182 spatial and temporal resolution. They do not, however, resolve the issue of basis risk, i.e.  
183 potential unfairness to insurance takers (Leblois, 2012). Moreover, the very nature of an  
184 index-based product creates the chance that an insured party may not be paid when they  
185 suffer loss. For this reason, in some countries (Spain) they have named this SIBI as  
186 “damaged in pasture” to cover not only drought even this one is the main cause.

187

188 It is highly recognized that shortage of water has many implications to agriculture,  
189 society, economy and ecosystems. Specifically, its impact on water supply, crop  
190 production and rearing of livestock is substantial in agriculture. Knowing the likelihood of  
191 drought is essential for impact prevention (Dalezios, 2013). Drought severity assessment  
192 can be approached in different ways: through conventional indices based on  
193 meteorological data, such as temperature, rainfall, moisture, etc. (Niemeyer, 2008), as  
194 well as through remote sensing indices based on images usually taken by artificial  
195 satellites (Lovejoy et al., 2008) or drones. In the second group they are found Satellite  
196 Vegetation Indices (SVI), which can quantify “green vegetation”, and soil moisture through  
197 Soil Water Index (Gouveia et al., 2009) combining different spectral reflectances. Thus,  
198 they are one of the main ways to quantitatively assess drought severity.

199

200 At the present time, several satellites (NOAA, TERRA, DEIMOS, etc.) can provide this  
201 spectral information with different spatial resolution. Some series with a high temporal  
202 frequency are freely available, those from NOAA satellites and Terra. The most widely  
203 known SVI is the Normalized Difference Vegetation Index (NDVI). It follows the principle  
204 that healthy vegetation mainly reflects the near-infrared frequency band. There are  
205 several other important SVI, such as Soil Adjusted Vegetation Index (SAVI) and Enhanced  
206 Vegetation Index (EVI) that incorporate soil effects and atmospheric impacts, respectively.  
207 An important point of SIBI is “when damage occurs”. To measure this, a SVI threshold  
208 value is defined mainly based on statistics that apply to Normal distributed variables:  
209 average and standard deviation. When current SVI values are bellow this threshold value  
210 for a period of time, insurance recognizes that a damage is occurring, most of the times  
211 drought, and then it begins to pay compensations to farmers.

212

213 Important NDVI-based indices of detecting drought are NDVI anomalies (NDVIA) and  
214 Standardized Vegetation Index (SVI). NDVIA and SVI have been successfully used to  
215 monitor drought conditions over different regions on the world (Nanzad et al., 2019; Li et  
216 al., 2014). NDVIA is calculated as the difference between the NDVI value for a specific time  
217 period (e.g., week, month) and the long-term mean value for that period. SVI was  
218 developed by Peters et al. (2002) and obtains the probability from normal NDVI  
219 distributions over multiple years of data, on a time period (Anyamba and Tucker, 2012;  
220 Bayarjargal et al., 2006). It is defined as:

221

$$222 \quad SVI_i = \frac{NDVI_i - \overline{NDVI}}{\sigma_{NDVI}} = \frac{NDVIA_i}{\sigma_{NDVI}} \quad (1)$$

223

224 where  $\overline{NDVI}$  is the long-term mean NDVI in the period  $i$ ,  $\sigma_{NDVI}$  is the standard deviation  
225 of NDVI in the period  $i$ , and  $NDVI_i$  is the current NDVI value in the time period  $i$ . Using

226 only the first and second statistical moment, average and the square root of variance,  
227 assumption of normality is implicit in this type of drought NDVI indicator.

228

229 WIBI aims to protect farmers against weather-based disasters such as droughts, frosts  
230 and floods. A WIBI policy links possible insurance payouts with the weather requirements  
231 of the crop being insured: the insurer pays an indemnity whenever the realized value of  
232 the weather index meets a specified threshold. Whereas payouts in traditional insurance  
233 programs are related to actual crop damages, a farmer insured under a WIBI contract may  
234 receive a payout. A current difficulty to the wide implementation of WIBI is the weakness  
235 of indices. Indeed, there is certainly a need for more efficient indices based on the  
236 additional experience gained from the implementation of WIBI products in the developing  
237 world. Current trends in index technology are exciting and they actuate high expectations,  
238 especially the development of yield indices and the use of remote sensing inputs. Risk  
239 protection and insurance illiteracy constitute another difficulty, which has to be addressed  
240 by training and awareness-raising at all levels, from farmers to farmers' associations,  
241 micro-insurance partners, as well as senior decision-makers in insurance, banking, and  
242 politics (Bailey, 2013). It is essential that all stakeholders (especially the insured) perfectly  
243 understand the principles of IBI, as otherwise the insurer, even the whole concept of  
244 insurance, is at risk of reputation loss for years or decades.

245

246 There is currently a lack of technical capacity in the insurance sectors of most  
247 developing countries, which is a constraint to the scaling up and further development of  
248 WIBI (Gommes and Kayitakire, 2012). Specifically, although it is possible to design an index  
249 product and assist in roll-out, marketing, and sales, such assistance is not possible on a  
250 wide scale, simply because there is lack of qualified expertise. Indeed, it usually requires  
251 mathematical modeling, data manipulation, and expertise in crop simulation to design an  
252 index. Nevertheless, it is possible to structure insurance with multiple indices, but this  
253 increases the complexity of the product and makes it difficult for farmers to comprehend  
254 it. 'Basis risk' is also a particular problem for index products, which is frequently caused by  
255 the fact that measurements of a particular variable, such as rain, may differ at the  
256 insurer's measurement site and in the farmer's field. This also creates problems for  
257 insurance providers. Indeed, part of the reason the scaling up of index products has failed  
258 is that both insurers and farmers suffer from this basis risk.

259

260 Currently, to mitigate impacts of climate-related reduced productivity of French  
261 grasslands, several studies have been developed to design new insurance scheme bases  
262 indemnity payouts to farmers on a forage production index (FPI) (Rumiguié et al., 2015;  
263 2017). Two examples of SIBIs are presented in two different countries: USA and Spain. In



264 particular, in USA there are several insurance programs for pasture, rangeland and forage,  
265 which use various indexing systems (rainfall and vegetation indices), and are promoted by  
266 Unites States Department of Agriculture (USDA) (Maples et al., 2016; USDA, 2018). NDVI is  
267 the index chosen in the vegetation index program and it is obtained from AVHRR  
268 (Advanced Very High Resolution Radiometer) sensor onboard NOAA satellites. Average,  
269 maximum and minimum NDVI values are obtained from a historical series with the aim of  
270 calculating a trigger value. Insurer decides the quantity of compensation comparing this  
271 trigger with current value. On the other hand, in Spain there exists the “Insurance for  
272 Damaged Pasture” from “Spanish System of Agricultural Insurance” (BOE, 2013). This  
273 insurance defines damage event through NDVI values obtained from MODIS sensor  
274 onboard TERRA satellite of NASA. In this insurance, NDVI threshold values ( $NDVI_{th}$ ) are  
275 calculated subtracting several times ( $k = 0.7$  or  $k = 1.5$ ) standard deviation to average  
276 within a homogeneous area:

277

$$278 \quad NDVI_{th} = \mu - k \cdot \sigma \quad (2)$$

279

280 where  $\mu, \sigma$  are average and standard deviation of NDVI respectively. Average and standard  
281 deviation come of supposing Normal distributions in the historical data (Goward et al.,  
282 1985; Hobbs, 1995; Fuller, 1998; Al-Bakri and Taylor, 2003; Turvey et al., 2012; De Leeuw  
283 et al. 2014).

284

285 The aim of this paper is to find a more realistic statistical NDVI distribution without  
286 the “a priori” assumption that variables follow a Normal distribution, typically for current  
287 SIBI methodology. In order to achieve this, the Maximum Likelihood Method (MLM) is  
288 fitted to a historical series of NDVI values in a pasture land area in Spain (Community of  
289 Madrid). Different types of asymmetrical distributions are examined with the aim to find a  
290 better fit than Normal. To eliminate some noise in the historical series, an original method  
291 is applied consisting of using Hue-Saturation-Lightness (HSL) color model. Finally, Chi-  
292 square test ( $\chi^2$  test) has been used to check the goodness of fit for all considered  
293 distributions.

294

295

## 296 **2. Materials and Methods**

### 297 **2.1 Vegetation Index**

298 The differences of the reflectance of green vegetation in parts of the electromagnetic  
299 radiation spectrum, namely, visible and near infrared, provide an innovative method for

300 monitoring surface vegetation from space. Specifically, the spectral behavior of vegetation  
301 cover in the visible (0.4-0.7mm) and near infrared (0.74-1.1mm, 1.3-2.5mm) offers the  
302 possibility to monitor from space the changes in the different stages of cultivated and  
303 uncultivated plants taking also into account the corresponding behavior of the  
304 surrounding microenvironment (Ortega-Farias et al., 2016). Indeed, from the visible part  
305 of the electromagnetic radiation spectrum it is possible to draw conclusions about the  
306 rate photosynthesis, whereas from near infrared inferences are extracted about the  
307 chlorophyll density and the amount of canopy in the plant mass, as well as the water  
308 content in the leaves, which is also linked directly to the rate of transpiration with impacts  
309 to physiological process of photosynthesis. Usually, data from NOAA/AVHRR series of  
310 polar orbit meteorological satellites are used with low spatial resolution (1.1 km<sup>2</sup>) and  
311 recurrence interval at least twice daily from the same location. Several algorithms  
312 combining channels of red (RED), near infrared (NIR) and green (GREEN) have been  
313 proposed, which provide indices sensitive to green vegetation.

314

315 NDVI uses two frequency bands: red band (660 nm) and near-infrared band (860 nm).  
316 Absorption of red band is related to photosynthetic activity and reflectance of near-  
317 infrared band is related to presence of vegetation canopies (Flynn, 2006). In drought  
318 periods, NDVI values can reduce significantly, therefore many researchers have used this  
319 index to measure drought events in recent years (Dalezios et al., 2014). To calculate NDVI  
320 we will use this mathematical formula:

321

$$322 \quad NDVI = \frac{IR-R}{IR+R} \quad (3)$$

323

324 where “IR” and “R” are reflectance values in Near-Infrared band and Red band,  
325 respectively. NDVI values below zero indicate no photosynthetic activity and are  
326 characteristic of areas with large accumulation of water, such as rivers, lakes, or  
327 reservoirs. The higher is the NDVI value, the greater is the photosynthetic activity and  
328 vegetation canopies.

329

330 In this paper, the NDVI is used, which is widely known index with a multitude of  
331 applications over time. The NDVI is suited for monitoring of total vegetation, since it partly  
332 compensates the changes in light conditions, land slope and field of view (Kundu et al.,  
333 2016). In addition, clouds, water and snow show higher reflectance in the visible than in  
334 the near infrared, thus, they have negative NDVI values. Indeed, bare and rocky terrain  
335 show vegetation index values close to zero. Moreover, the NDVI constitutes a measure of  
336 the degree of absorption by chlorophyll in the red band of the electromagnetic spectrum.

337 In summary, the NDVI is a reliable index of the chlorophyll density on the leaves, as well as  
338 the percentage of the leaf area density over land, thus, NDVI constitutes a credible  
339 measure for the assessment of dry matter (biomass) in various species vegetation cover  
340 (Dalezios, 2013). It is clear from the above that the NDVI is an index closely related to  
341 growth and development of plants, which can effectively monitor surface vegetation from  
342 space.

343

344 The continuous increase of the NDVI value during the growing season reflects the  
345 vegetative and reproductive growth due to intense photosynthetic activity, as well as the  
346 satisfactory correlation with the final biomass production at the end of a growing period.  
347 On the other hand, gradual decrease of the NDVI values signifies stress due to lack of  
348 water or extremely high temperatures for the plants, leading to a reduction of the  
349 photosynthetic rate and ultimately a qualitative and quantitative degradation of plants.  
350 NDVI values above zero indicate the existence of green vegetation (chlorophyll), or bare  
351 soil (values around zero), whereas values below zero indicate the existence of water,  
352 snow, ice and clouds.

353

## 354 **2.2 Database**

355 Scientific research satellite Terra (EOS AM-1) has been chosen to provide necessary  
356 information to calculate NDVI in the study area. This satellite was launched into orbit by  
357 NASA on December 18, 1999. MODIS sensor aboard this satellite collects information of  
358 different reflectance bands. MODIS information is organized by "products". The product  
359 used in this study was MOD09A1 (LP DAAC, 2014). MOD09A1 incorporates seven  
360 frequency bands: Band 1 (620-670 nm), band 2 (841-876 nm), band 3 (459-479 nm), band  
361 4 (545-565 nm), 5 band (1230-1250 nm), band 6 (1628-1652 nm) and band 7 (2105-2155  
362 nm). The bands used to calculate NDVI are: band 1 for red frequency and band 2 for near-  
363 infrared frequency. MOD09A1 provides georeferenced images with pixel resolution of  
364 500m x 500m. Each MOD09A1 pixel contains the best possible L2G observation during an  
365 8-day period as selected on the basis of high observation coverage, low view angle, the  
366 absence of clouds or cloud shadow, and aerosol loading.

367

368 The period of time selected on this study was from 2002 to 2017.

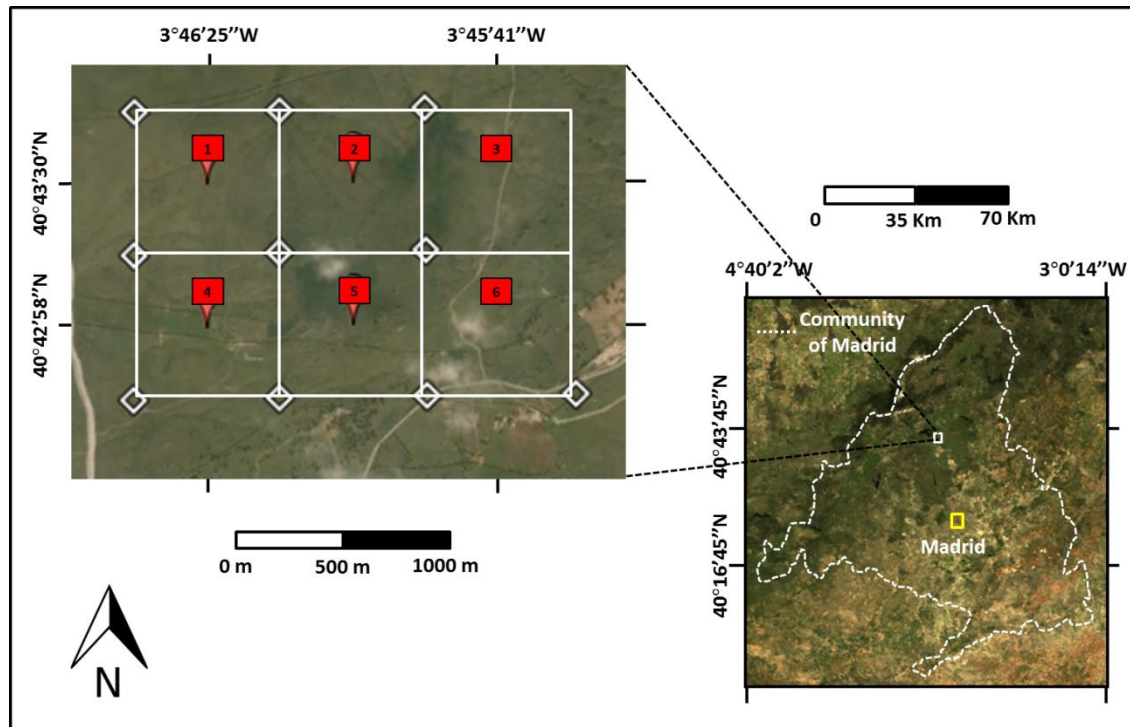
369

370 Daily data from a principal station of the meteorological network were utilized during  
371 the period studied (2002 – 2017). Meteorological station is located in 40°41'46"N  
372 3°45'54"W (elevation 1004 m a.s.l.), less than 2 km from the study area (AEMET, 2017).

373

374 **2.3 Site description**

375 Six pixels (500m x 500m) are considered located in a pasture area at the north of the  
376 Community of Madrid (Spain) between the municipalities of "Soto del Real" and  
377 "Colmenar Viejo". The study area is located between meridians 3° 45' 00" and 3° 47' 00"  
378 W and parallels 40° 42' 00" and 40° 44' 00" N approximately (see Fig. 1).  
379



380  
381 **Figure 1.** The study area is in the centre of the Iberian Peninsula (Community of Madrid). RGB  
382 image of six pixels area used for case study is shown (Google Earth's and MODIS images).

383  
384 The annual mean temperature ranges during the study period from 12.7°C to 13.8°C,  
385 and annual mean precipitation ranges from 360 mm to 781 mm. The stations studied  
386 were identified semi-arid (annual ratio P/ETo between 0.2 and 0.5) according to the global  
387 aridity index developed by the United-Nations Convention to Combat Desertification  
388 (UNEP, 1997). According to the climatic classification of Köppen (Kottek et al., 2006), this  
389 area presents a continental Mediterranean climate temperate with dry and temperate  
390 summer (type Csb). Temperature and precipitation of this site, based on 20 years, is  
391 presented in Table 1.

392  
393 Due to high soil moisture conditions, ash is the dominant tree, forming large  
394 agroforestry systems ("dehesas") that are used for pasture. These are ecosystems with  
395 high biodiversity.

396

397 **Table 1.** Monthly average of maximum temperature (Tmax), average temperature (Tavg),  
398 minimum temperature (Tmin) and precipitation (P). Study period from 1997 to 2017.

Month	Jan	Feb	Mar	Apr	May	Jun	Jul	Aug	Sep	Oct	Nov	Dec	Annual
Tmax (°C)	7.1	9.3	12.7	15.4	19.5	24.6	28.6	28.1	23.7	16.8	11.1	7.4	17.0
Tavg (°C)	3.6	4.8	7.7	10.1	13.7	18.4	22.0	21.7	17.9	12.3	7.1	4.1	12.0
Tmin (°C)	0.0	0.3	2.6	4.8	7.8	12.1	15.4	15.3	12.0	7.8	3.0	0.8	6.8
P (mm)	67.2	50.0	38.5	62.2	62.3	30.2	18.9	16.4	34.2	79.3	86.2	82.6	627.9

399

#### 400 **2.4 HSL model**

401 There is no doubt that NDVI time-series from satellite sensors carry useful  
402 information, which can be used for characterizing seasonal dynamics of vegetation  
403 (Fensholt et al., 2012; Forkel et al., 2013). However, due to unfavorable atmospheric  
404 conditions during the data acquisition, NDVI time-series curve often contains noise  
405 (Motohka et al., 2011; Park, 2013). Although most of the NDVI data products are  
406 temporally composited through maximum value compositing (MVC) method (Holben,  
407 1986) to retain relatively cloud-free data, residual noise still exists in the data, which will  
408 affect the accuracy of the NDVI value.

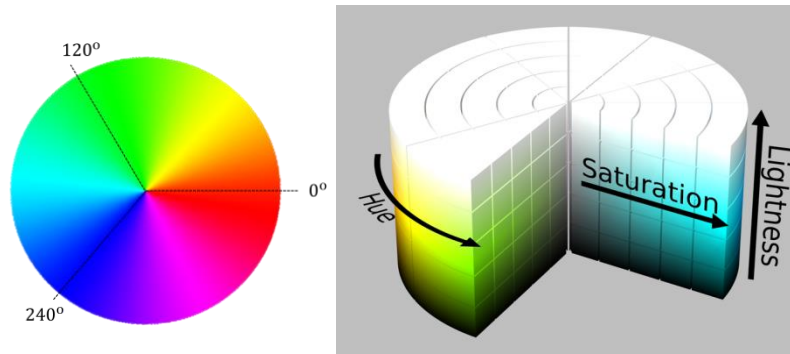
409

410 Therefore, usually it is necessary to reconstruct of NDVI time-series before extracting  
411 information from the noisy data. There are several techniques that have been applied to  
412 reduce noise and reconstruct NDVI series, a summary of these can be found in Wei et al.  
413 (2016). In this study we applied a simple filtering method based on the Hue-Saturation-  
414 Lightness (HSL) color model inspired by the work presented by Tackenberg (2007).

415

416 HSL color model is a cylindrical representation of RGB (Red-Green-Blue) points. Their  
417 components are Hue (color type), Saturation (level of color purity) and Lightness (color  
418 luminosity). Hue is the angular component and it is more intuitive for humans since it is  
419 directly related to the color wheel (see Fig. 2).

420



421  
422 **Figure 2.** Colour wheel of Hue (on the left) and the HSL model (on the right).

423 Saturation is the radial component and near-zero values indicate grey colors.  
424 Lightness is the axial radial versus axial component, zero lightness produces black and  
425 lightness produces white.

426  
427 The NDVI series are filtered using the following HSL criterion: NDVI values are valid if  
428 HSL Saturation is greater than 0.15. In this way, the values of the series that have grey  
429 color correlate with pasture covered by clouds or snow are eliminated. This type of filter  
430 based in HSL color space has been used on digital camera images monitoring vegetation  
431 phenology (Tackenberg, 2007; Crimmins and Crimmins, 2008; Graham et al., 2009).  
432 However, we have not found the use of this HSL criterion in the context of NDVI remote  
433 sensing images.

## 434 435 **2.5 Maximum Likelihood Method**

436 MLM estimates the set of parameters  $\{\alpha, \beta, \mu, \sigma, \dots\}$  for a specific statistical  
437 distribution that maximizes the “likelihood function” or the “joint density function”:

$$438 \quad L = f(\mathbf{x}, \boldsymbol{\theta}) = \prod_{i=1}^n f(x_i; \alpha, \beta, \mu, \sigma, \dots) \quad (4)$$

439 where  $\mathbf{x} = (x_1, \dots, x_n)$  is the set of data,  $\boldsymbol{\theta} = (\alpha, \beta, \mu, \sigma, \dots)$  is the vector of parameters  
440 and  $f(x_i; \alpha, \beta, \mu, \sigma, \dots)$  is the density function of the statistical model.

441 When maximization with respect to the vector of parameters is carried out, the  
442 estimated parameters  $(\hat{\alpha}, \hat{\beta}, \hat{\mu}, \hat{\sigma}, \dots)$  for the proposed statistical distribution are obtained  
443 (Larson, 1982). Properties of estimated parameters are: invariance, consistency and  
444 asymptotically unbiased.

445 In the case of a Normal model, the estimated statistics  $\mu$  and  $\sigma$  are defined by  
446 accurate expressions as follows:

447 
$$\hat{\mu} = \bar{x} = \frac{1}{n} \sum_{i=1}^n x_i \quad \hat{\sigma} = s = \sqrt{\frac{1}{n} \sum_{i=1}^n (x_i - \bar{x})^2} \quad (5)$$

448 where  $\hat{\mu}$  is the sample mean and  $\hat{\sigma}$  is the sample standard deviation of the data set.

449 In this study we will apply MLM to estimate the parameters for 4 probability density  
 450 functions (PDF). In Table 2, a brief description is presented of these PDF candidates:  
 451 Normal, Gamma, Beta and GEV. To do so, the following MATLAB functions have been  
 452 used: “normfit”, “gamfit”, “betafit” and “gevfit” (respectively).  
 453

454 **Table 2.** Candidate Probability Density Functions (PDF).

PDF NAME	PDF EXPRESSION	PDF PARAMETERS
Normal	$f(x; \mu, \sigma) = \frac{1}{\sigma\sqrt{2\pi}} e^{-\frac{1}{2}\left(\frac{x-\mu}{\sigma}\right)^2}$	$\mu \equiv \textit{average}$ $\sigma \equiv \textit{standard deviation}$
Gamma	$f(x; \alpha, \beta) = \frac{1}{\beta^\alpha \Gamma(\alpha)} x^{\alpha-1} e^{-\frac{x}{\beta}}$	$\Gamma(\cdot) \equiv \textit{gamma function}$ $\alpha \textit{ and } \beta \equiv \textit{parameters}$
Beta	$f(x; a, b) = \frac{\Gamma(a+b)}{\Gamma(a)\Gamma(b)} x^{a-1} (1-x)^{b-1}$	$\Gamma(\cdot) \equiv \textit{gamma function}$ $a \textit{ and } b \equiv \textit{parameters}$
GEV	$f(x; \mu, \sigma, \xi) = \frac{1}{\sigma} t(x)^{\xi+1} e^{-t(x)}$ where $t(x) = \begin{cases} \left(1 + \left(\frac{x-\mu}{\sigma}\right)\xi\right)^{-1/\xi} & \text{if } \xi \neq 0 \\ e^{-(x-\mu)/\sigma} & \text{if } \xi = 0 \end{cases}$	$\mu \in \mathbb{R} \equiv \textit{location param.}$ $\sigma > 0 \equiv \textit{scale parameter}$ $\xi \in \mathbb{R} \equiv \textit{shape parameter}$

455

456

## 457 2.6 Goodness of fit (Chi square test)

458  $\chi^2$  test can be used to determine to what extent observed frequencies differ from  
 459 frequencies expected for a specific statistical model. The most important points of the  
 460 theory are briefly presented in (Cochran, 1952).  
 461

462

463 Let  $f(x, \theta)$  be a theoretical density function of a random variable X which depends on  
 464 parameters  $\theta = (\alpha, \beta, \mu, \sigma, \dots)$  and let  $x_1, \dots, x_n$  be a sample of X grouped into k classes with  $n_i$   
 465 data per class i.

466

467 Firstly, the following hypothesis is set:

468

469  $(H_0)$  observed data fit theoretical distribution  $f(x, \theta)$ .

470 Then the test statistic  $\chi_c^2$  is defined as:

470 
$$\chi_c^2 = \sum_{i=0}^k \frac{(n_i - e_i)^2}{e_i} \quad (6)$$

471 where  $n_i$  is the number of data or observed frequency and  $e_i = n \cdot P(\text{class } i)$  is the  
 472 expected frequency for class  $i$ .  $P(\text{class } i)$  is the theoretical interval probability defined for  
 473 class  $i$ .

474 A level of significance is also set as:

475 
$$\alpha = P(\text{Reject } H_0 / H_0 \text{ is true}) \quad (7)$$

476 Finally, the following decision rule is applied: “reject the theoretical distribution at  
 477 significance level  $\alpha$  if:

478 
$$\chi_c^2 > \chi_{(k-m-1, 1-\alpha)}^2 \quad (8)$$

479 where  $\chi_{(k-m-1, 1-\alpha)}^2$  is a  $\chi^2$  distribution with  $k-m-1$  degrees of freedom ( $m$  is the number of  
 480 parameters,  $k$  is the number of classes).

481  
 482

### 483 **3. Results**

#### 484 **3.1 HSL filtering criterion**

485 NDVI series (from 2002 to 2017) were obtained for each pixel of the study area using  
 486 frequency bands provided by MODIS product named MOD09A1. These series contain  
 487 some irregular values that can skew NDVI pattern. Therefore, the six series (six pixels)  
 488 were filtered using the HSL criterion.

489

490 MOD09A1 is a MODIS product that processes data to obtain the best observation in  
 491 an 8-days period. However, it is possible that the result of this selection still presents  
 492 some problems since the best of this selection is relative to the eight observations of the  
 493 period. For example, if the eight observations, at one pixel, appear with clouds, shadow  
 494 clouds or snow, the best selection still maintains this problem.

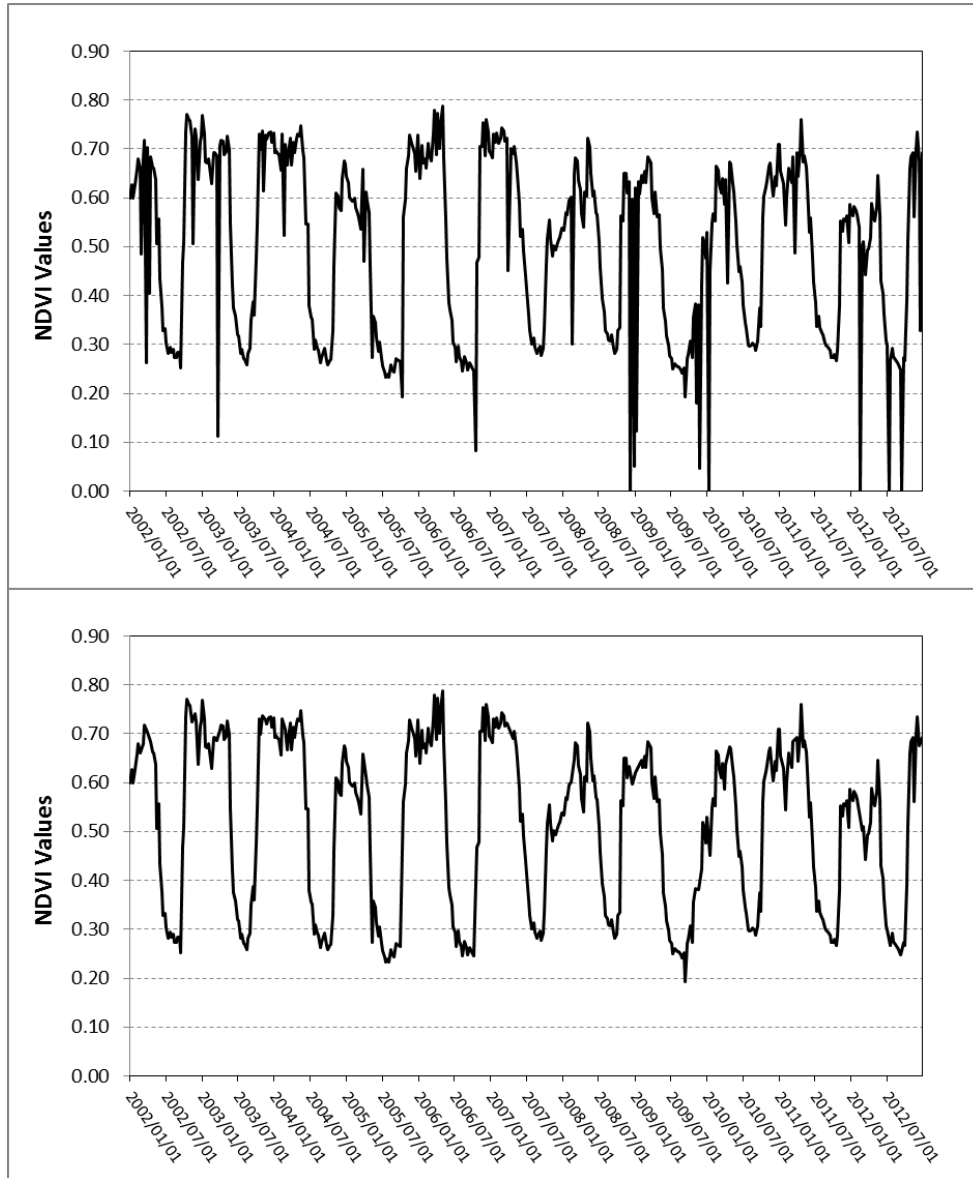
495

496 As an example of above, the NDVI series (10 years) of one pixel of the study area is  
 497 shown in Fig. 3. On the top graph of Fig. 3 it is noticed that there exit some extremely low  
 498 NDVI values in some dates. If these NDVI values are compared to neighbor values (8 days  
 499 after or before) the high variation presented in such short period is not believable. This  
 500 issue tells us that MODIS sensor has not obtained a proper observation in this 8 days  
 501 period (interval).



502  
503  
504  
505  
506  
507

HSL criterion helps us to eliminate these incorrect NDVI values, since the filter is interpreting that these pixels still contains clouds or snow, i.e., pixels with low saturation (greyish colours).



508  
509  
510

**Figure 3.** HSL filtering criterion applied to a 10 years NDVI series. Top graph shows the real NDVI series. Bottom graph shows the HSL filtered NDVI series.

511  
512  
513

Fig. 3 shows that abrupt changes in the NDVI values, mainly observed during raining seasons such as autumn and winter, are efficiently eliminated. Not to be a high computational demanding method is one of the main advantages of HSL filtering method.

514 Therefore, this method will allow us to obtain more robust NDVI values to be used in the  
 515 statistical analysis.  
 516

517 **3.2 Statistical analysis**

518 NDVI values were obtained consecutively every 8 days from MODIS product starting  
 519 at the 1<sup>st</sup> of January of every year, in such a way that 46 NDVI observations were extracted  
 520 for each year. Therefore, it was possible to define 46 Random Variables (RV) when all the  
 521 years of this study were taking into account.

522 In Table 3, every RV (named as “Interval”) is shown together with the number of  
 523 available NDVI observations. Each RV collects the observations coming from the six  
 524 selected pixels; therefore the maximum number of observations per RV could be: 6 pixels  
 525 x 16 years = 96 observations. The start intervals of each season are: interval 45 (19  
 526 December) for winter, interval 11 (22 March) for spring, interval 23 (26 June) for summer  
 527 and interval 34 (22 September) for autumn.  
 528

529 **Table 3.** Number of observations for every RV (named as Interval).

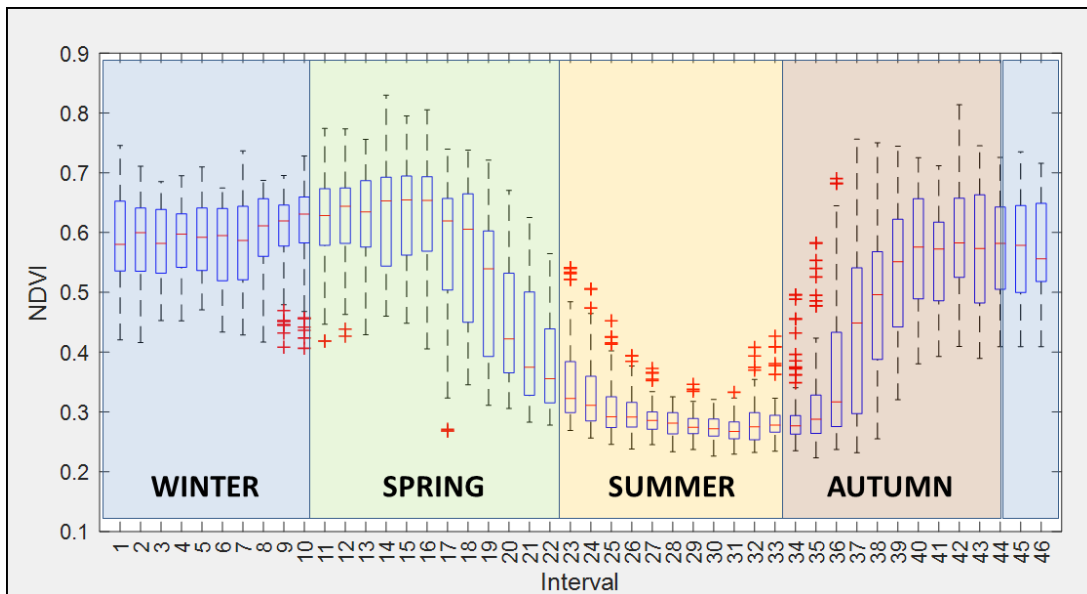
RANDOM VARIABLE	# OBSERVATIONS	RANDOM VARIABLE	# OBSERVATIONS
Interval 1	85	Interval 24	96
Interval 2	84	Interval 25	96
Interval 3	96	Interval 26	96
Interval 4	96	Interval 27	96
Interval 5	95	Interval 28	96
Interval 6	90	Interval 29	96
Interval 7	86	Interval 30	96
Interval 8	83	Interval 31	96
Interval 9	96	Interval 32	96
Interval 10	96	Interval 33	94
Interval 11	74	Interval 34	96
Interval 12	88	Interval 35	96
Interval 13	88	Interval 36	85
Interval 14	88	Interval 37	90
Interval 15	96	Interval 38	96
Interval 16	92	Interval 39	92
Interval 17	88	Interval 40	90
Interval 18	96	Interval 41	96
Interval 19	95	Interval 42	89
Interval 20	96	Interval 43	95

<b>Interval 21</b>	95
<b>Interval 22</b>	96
<b>Interval 23</b>	96

<b>Interval 44</b>	88
<b>Interval 45</b>	90
<b>Interval 46</b>	90

530  
531  
532  
533  
534  
535

In Fig. 4, box plots of all RV with a start and end reference of the astronomical seasons are shown. The typical evolution of the NDVI along a year can be seen together with the inter-quartile range.



536  
537  
538

**Figure 4.** Box plots of 46 random variables (RV) are shown as well as start and end reference of every season. Study period from 2002 to 2017.

539  
540  
541  
542  
543  
544  
545

The observed evolution of NDVI through the different seasons is typical of the pasture in this area. The summer presents the lowest mean values which begin to increase in autumn achieving a maximum mean value of 0.60 or 0.65 during the beginning of spring. In the middle of the spring NDVI decrease again, approaching the lowest mean value of 0.28 approximately in summer.

546  
547  
548  
549  
550

Taking into account these values, dense vegetation, in this study pasture, is found from middle of October (interval 37) till the end of May (interval 19). It is in this period where the precipitation concentrates (see Table 1). During the summer, the NDVI mean values are lower than 0.3 corresponding with low precipitation and high temperatures.

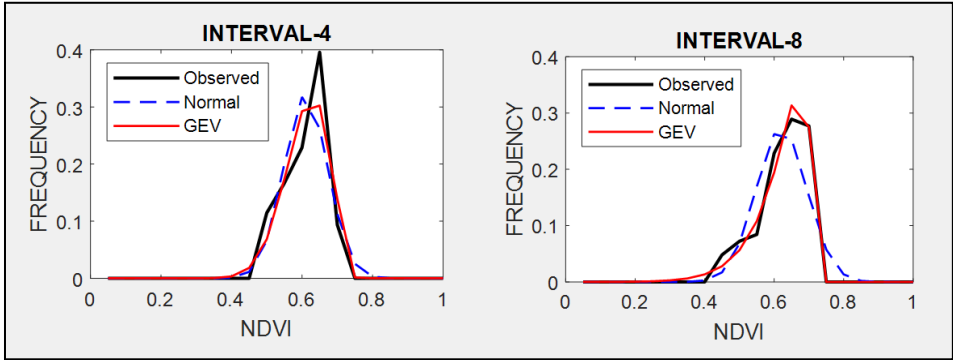
551 Following the work of Escribano-Rodriguez et al. (2014), there is a relationship of  
552 pasture damage and a NDVI value around 0.40. Even if the authors point out that this  
553 value is highly variable depending on the location, we can see that summer season in this  
554 case study is under this value (see Fig. 4). This can explain that “Insurances for Damaged  
555 Pasture” usually do not apply in these dates due to the arid environment (BOE, 2013).

556  
557 The statistical metric used in this study to assess the fit of the observed NDVI values  
558 with respect to the PDF candidates (Normal, Gamma, Beta and GEV) was the Chi square  
559 test ( $\chi^2$  test). The following steps were carried out:

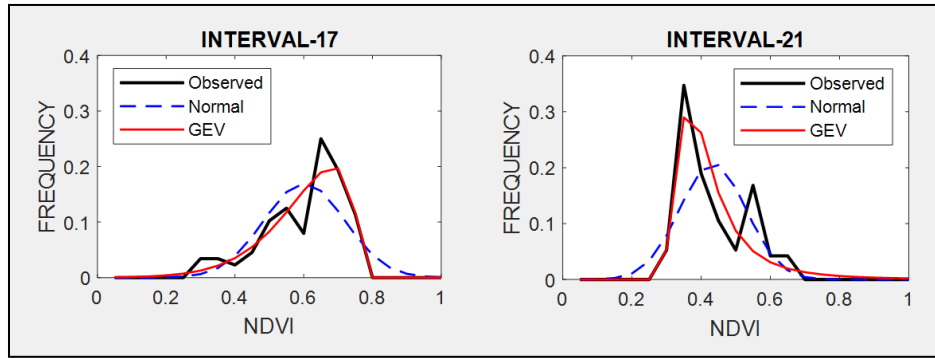
- 560
- 561 3. MLM was applied to model these 46 RV. Parameters were calculated for the four  
562 PDF candidates (see Table 2).
- 563 4. To check the goodness of the fit of PDF candidates, Chi square test ( $\chi^2$  test) was  
564 applied from 7 classes to 14 classes meeting the requirement that each class has  
565 at least five observations. The level of significance ( $\alpha$ ) was fixed to 5% for all the  
566 candidates.
- 567

568 **3.2.1 Maximum Likelihood Method**

569 Table A1 at Appendix A shows the estimated parameters for each PDF and each  
570 interval calculated by the MLM. These parameters were used to compare the estimated  
571 PDF with the NDVI observed values on different times through the seasons. The following  
572 intervals are shown as examples of better GEV fit: interval 4 and 8 (for winter, see Fig. 5),  
573 interval 17 and 21 (for spring, see Fig. 6) and interval 36 and 40 (for autumn, see Fig. 7). In  
574 these plots, observed frequency is compared versus Normal and GEV density distributions  
575 calculated by MLM.



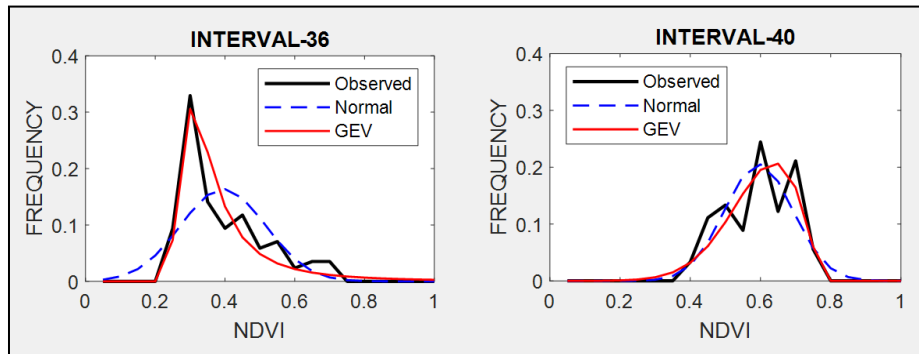
577  
578 **Figure 5.** Comparison between observed NDVI frequency, GEV and Normal probability density  
579 functions (PDF) on two different dates. Intervals 4 and 8 are examples for winter.



580

581 **Figure 6.** Comparison between observed NDVI frequency, GEV and Normal probability density  
 582 functions (PDF) on two different dates. Intervals 17 and 21 are examples for spring.

583



584

585 **Figure 7.** Comparison between observed NDVI frequency, GEV and Normal probability density  
 586 functions (PDF) on two different times. Intervals 36 and 41 are examples for autumn.

587

588 During winter (see Fig. 5) the observed NDVI distribution presents negative skewness.  
 589 Then, there is a higher frequency of high NDVI values corresponding with significant  
 590 precipitation. During spring (see Fig. 6) an evolution in the skewness is observed passing  
 591 from negative to positive, and so, the lower NDVI values become the higher probable.  
 592 Finally, during autumn (see Fig. 7) precipitation begins and from positive pass to negative  
 593 skewness and higher NDVI values are possible. We can observe that Normal distribution  
 594 has no flexibility to follow this dynamic in the distributions on each time. This comparison  
 595 is done in a sequential order for the whole of intervals in Figures A1, A2, A3 and A4 at  
 596 Appendix A.

597

### 598 **3.2.2 Chi square test**

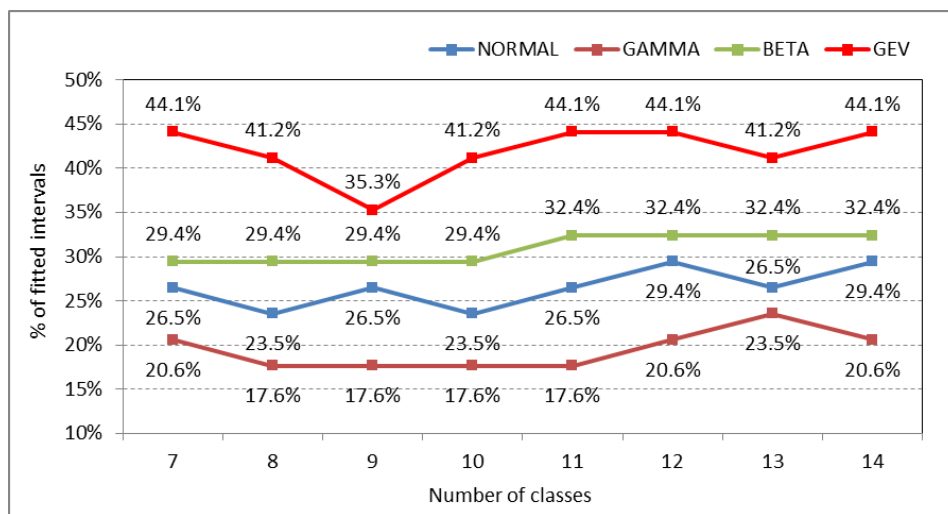
599 Twelve intervals (from 23 to 34) corresponding to months of July, August and  
 600 September have been excluded of this analysis since these intervals fall into the dry

601 season in the study area, normally not cover by any SIBI. Therefore, calculations were  
 602 carried out over 34 intervals.

603

604 To assess the general goodness of fit, the number of intervals where the  $\chi^2$  test was  
 605 accepted (or failed to reject) was calculated for every PDF candidate. Then, the  
 606 percentage of accepted intervals, over the total 34 intervals, was also calculated (the  
 607 quality estimator). Fig. 8 shows this percentage of intervals that fit for every PDF  
 608 candidate. The number of classes used in  $\chi^2$  test is represented at X-axis (from 7 to 14  
 609 classes).

610



611

612 **Figure 8.** Percentage of fitted intervals (Y axis) for each PDF candidate (Normal, Gamma, Beta and  
 613 GEV distributions) in function of the number of classes (X axis).

614

## 615 4. Discussion

### 616 4.1 Statistical context

617 Fig. 8 indicates that GEV distributions explain more intervals (more than 40% for the  
 618 majority of the class analysis) than Normal, Gamma or Beta distributions. An important  
 619 difference between the Normal distribution and the rest of the PDF used in this work is its  
 620 skewness and kurtosis. Many of the observed NDVI distributions present a clear  
 621 asymmetry and long tails in one or both sides that causes Normal distribution not to be  
 622 the optimal fit.

623

624 There is a relationship between seasons and the number of intervals that fit correctly.  
 625 We found that GEV distributions explain better intervals of spring and autumn since their

626 observed distributions are very asymmetric. On the other hand, we did not find an  
627 important difference in winter, since its observed distributions are mainly symmetric.

628

629 The more skewness and kurtosis depart from those of the Normal distribution the  
630 larger the errors affecting the insurance designed based on (Turvey et al., 2012). It is an  
631 expected result as pasture scenario is quite different from the development of a crop,  
632 where Normal distributions in the NDVI values are more expected. This high heterogeneity  
633 in time and space of NDVI estimated on pasture has been pointed out in several works  
634 (Martin-Sotoca et al, 2018). At the same time, more different is the observed NDVI  
635 frequency from a Normal distribution less representative is the average, and so, the  
636 median becomes a more representative value.

637

#### 638 **4.2 Insurance context**

639 The use of NDVI thresholds in damaged pasture context was presented in the  
640 introduction section, being an example of using the "Insurance for Damaged Pasture" in  
641 Spain. We have chosen this last insurance to compare the results between applying  
642 Normal and GEV distribution methodologies. In this particular case the NDVI threshold  
643 ( $NDVI_{th}$ ) was calculated using the expression  $NDVI_{th} = \mu - k \cdot \sigma$  (where  $\mu, \sigma$  are average  
644 and standard deviation of NDVI distributions respectively, assuming the Normal  
645 hypothesis).

646

647 The probability of being below  $NDVI_{th}$  (using  $k = 0.7$ , first damage level in the  
648 insurance) at every interval has been calculated assuming the Normal hypothesis. As it  
649 was expected, this value is always 24.2% (see third column in Table 4). The probability of  
650 being below  $NDVI_{th}$  has also been calculated using GEV distributions obtained in this  
651 study. The probability obtained by GEV distributions is mostly lower than the Normal  
652 distributions in spring, autumn and winter (see Table 4) that is the working period of the  
653 insurance.

654

655 Observing where in time are localized the highest relative error in probabilities (fifth  
656 column in Table 4), intervals corresponding to the end of winter, second middle of spring  
657 and the beginning of autumn present errors higher than 10%. This could explain why it is  
658 in spring and autumn when more disagreements exist between farmers and insurance  
659 company in claims.

660

661 **Table 4 – First column:** time intervals of approximately 8 days along the year. **Second column:** NDVI  
662 thresholds ( $NDVI_{th}$ ) based on a Normal distribution applying  $\mu - 0.7 \times \sigma$ . **Third column:** percentages of

663 area below the  $NDVI_{th}$  when Normal distributions are applied. **Fourth column:** percentages of area  
 664 below the  $NDVI_{th}$  when GEV distributions are applied. **Fifth column:** relative area error of GEV  
 665 compared to the Normal distribution.

666

RANDOM VARIABLE	NORMAL		GEV	
	$NDVI_{th}$	Prob.	Prob.	Error (%)
Interval 1	0.535	24.20%	24.37%	0.70%
Interval 2	0.541	24.20%	23.18%	-4.21%
Interval 3	0.541	24.20%	23.27%	-3.84%
Interval 4	0.543	24.20%	23.27%	-3.84%
Interval 5	0.545	24.20%	24.17%	-0.12%
Interval 6	0.534	24.20%	21.48%	-11.24%
Interval 7	0.528	24.20%	24.01%	-0.79%
Interval 8	0.546	24.20%	20.70%	-14.46%
Interval 9	0.555	24.20%	21.30%	-11.98%
Interval 10	0.561	24.20%	22.28%	-7.93%
Interval 11	0.567	24.20%	23.49%	-2.93%
Interval 12	0.572	24.20%	23.75%	-1.86%
Interval 13	0.571	24.20%	23.20%	-4.13%
Interval 14	0.570	24.20%	24.29%	0.37%
Interval 15	0.571	24.20%	23.47%	-3.02%
Interval 16	0.560	24.20%	23.26%	-3.88%
Interval 17	0.495	24.20%	21.29%	-12.02%
Interval 18	0.484	24.20%	21.58%	-10.83%
Interval 19	0.442	24.20%	23.06%	-4.71%
Interval 20	0.381	24.20%	27.20%	12.40%
Interval 21	0.342	24.20%	29.46%	21.74%
Interval 22	0.323	24.20%	28.84%	19.17%
Interval 35	0.257	24.20%	18.98%	-21.57%
Interval 36	0.285	24.20%	28.57%	18.06%
Interval 37	0.333	24.20%	25.90%	7.02%
Interval 38	0.398	24.20%	24.27%	0.29%
Interval 39	0.454	24.20%	23.79%	-1.69%
Interval 40	0.503	24.20%	22.81%	-5.74%
Interval 41	0.491	24.20%	23.23%	-4.01%
Interval 42	0.517	24.20%	24.66%	1.90%
Interval 43	0.507	24.20%	23.13%	-4.42%



<b>Interval 44</b>	0.514	24.20%	23.49%	-2.93%
<b>Interval 45</b>	0.515	24.20%	23.70%	-2.07%
<b>Interval 46</b>	0.509	24.20%	23.33%	-3.60%

667

668 An alternative calculation can be the use of Normal probability (24.2%) to calculate new  
669  $NDVI_{th}$  based on GEV (see Table 5). It can be seen that new  $NDVI_{th}$  obtained by GEV  
670 distributions are mostly upper than thresholds using Normal distributions in spring,  
671 autumn and winter. Considering these results we find that damage thresholds calculated  
672 by GEV methodology are mostly above that one's calculated by Normal methodology.

673 Again, intervals corresponding to the end of winter, second middle of spring and the  
674 beginning of autumn present  $NDVI_{th}$  relative errors higher than 1% in absolute values  
675 (fourth column in Table 5).

676

677 **Table 5 - First column:** time intervals of approximately 8 days along the year. **Second column:** NDVI  
678 thresholds ( $NDVI_{Th}$ ) based on a Normal distribution (Normal) applying  $\mu - 0.7 \times \sigma$ . **Third column:**  
679  $NDVI_{Th}$  based on a GEV distribution (GEV) using 24.2% as the area below the  $NDVI_{Th}$ . **Fourth column:**  
680 relative  $NDVI_{Th}$  error of GEV compared to the Normal distribution.

681

<b>RANDOM VARIABLE</b>	<b>NDVI<sub>Th</sub></b>		<b>Error (%)</b>
	<b>Normal</b>	<b>GEV</b>	
<b>Interval 1</b>	0.535	0.534	-0,19%
<b>Interval 2</b>	0.541	0.543	0,37%
<b>Interval 3</b>	0.541	0.543	0,37%
<b>Interval 4</b>	0.543	0.545	0,37%
<b>Interval 5</b>	0.545	0.545	0,00%
<b>Interval 6</b>	0.534	0.543	1,69%
<b>Interval 7</b>	0.528	0.528	0,00%
<b>Interval 8</b>	0.546	0.558	2,20%
<b>Interval 9</b>	0.555	0.563	1,44%
<b>Interval 10</b>	0.561	0.567	1,07%
<b>Interval 11</b>	0.567	0.569	0,35%
<b>Interval 12</b>	0.572	0.574	0,35%
<b>Interval 13</b>	0.571	0.574	0,53%
<b>Interval 14</b>	0.570	0.569	-0,18%
<b>Interval 15</b>	0.571	0.573	0,35%
<b>Interval 16</b>	0.560	0.563	0,54%

<b>Interval 17</b>	0.495	0.510	3,03%
<b>Interval 18</b>	0.484	0.498	2,89%
<b>Interval 19</b>	0.442	0.447	1,13%
<b>Interval 20</b>	0.381	0.374	-1,84%
<b>Interval 21</b>	0.342	0.334	-2,34%
<b>Interval 22</b>	0.323	0.318	-1,55%
<b>Interval 35</b>	0.257	0.262	1,95%
<b>Interval 36</b>	0.285	0.278	-2,46%
<b>Interval 37</b>	0.333	0.327	-1,80%
<b>Interval 38</b>	0.398	0.398	0,00%
<b>Interval 39</b>	0.454	0.455	0,22%
<b>Interval 40</b>	0.503	0.508	0,99%
<b>Interval 41</b>	0.491	0.494	0,61%
<b>Interval 42</b>	0.517	0.516	-0,19%
<b>Interval 43</b>	0.507	0.510	0,59%
<b>Interval 44</b>	0.514	0.516	0,39%
<b>Interval 45</b>	0.515	0.516	0,19%
<b>Interval 46</b>	0.509	0.511	0,39%

682

683

## 684 **5. Conclusions**

685 According to the results obtained in the study area using MLM and  $\chi^2$  test, it can be  
686 concluded that Normal distributions are not a good fit to the NDVI observations, and GEV  
687 distributions provide a better approximation.

688

689 The difference between Normal and GEV assumption is more evident in the transition  
690 from winter to summer (spring), where NDVI values decrease, and then from summer to  
691 winter (autumn) presenting the opposite behavior of increasing NDVI values. In both  
692 periods asymmetrical distributions were found, negative skewness for the spring  
693 transition and positive skewness for the autumn transition. During both periods the  
694 variability in precipitation and temperatures were higher in this location.

695

696 We have found differences if GEV assumption is selected instead of the Normal one  
697 when defining damaged pasture thresholds ( $NDVI_{th}$ ). The use of these different  
698 assumptions should be taken into account in future insurance implementations due to the  
699 important consequences of supposing a damage event or not. We propose the use of

700 quantiles in observed NDVI distributions instead of average and standard deviation,  
701 typically of Normal distributions, to calculate new  $NDVI_{th}$ .

702

703

704

## 705 **Acknowledgements**

706 This research has been partially supported by funding from MINECO under contract No.  
707 MTM2015-63914-P and CICYT PCIN-2014-080.

708

709 **Appendix A**

710

711

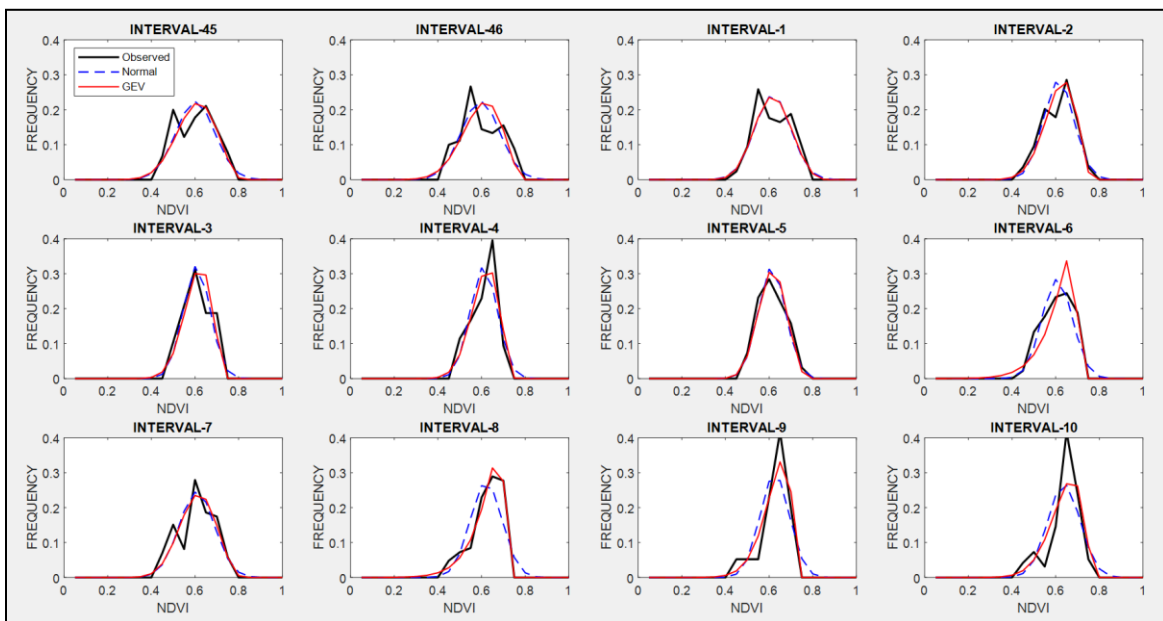
**Table A1** - Maximum Likelihood parameters calculated for 4 PDF.

RANDOM VARIABLE	NORMAL		GAMMA		BETA		GEV		
	$\mu$	$\sigma$	$\alpha$	$\beta$	a	b	$\mu$	$\sigma$	$\xi$
Interval 1	0.591	0.081	53.31	0.011	21.45	14.82	0.563	0.080	-0.297
Interval 2	0.589	0.069	71.14	0.008	30.62	21.40	0.571	0.073	-0.477
Interval 3	0.583	0.060	94.15	0.006	39.56	28.34	0.567	0.063	-0.457
Interval 4	0.585	0.060	91.88	0.006	39.58	28.05	0.570	0.064	-0.468
Interval 5	0.588	0.061	93.92	0.006	38.83	27.25	0.568	0.061	-0.340
Interval 6	0.582	0.068	70.28	0.008	30.67	22.05	0.577	0.083	-0.846
Interval 7	0.584	0.080	52.52	0.011	22.16	15.82	0.559	0.082	-0.366
Interval 8	0.596	0.071	65.37	0.009	28.89	19.59	0.591	0.081	-0.833
Interval 9	0.601	0.066	76.02	0.008	34.31	22.84	0.590	0.070	-0.652
Interval 10	0.613	0.073	63.83	0.010	27.80	17.62	0.598	0.079	-0.572
Interval 11	0.621	0.078	58.72	0.011	24.33	14.86	0.600	0.083	-0.451
Interval 12	0.624	0.073	68.33	0.009	28.01	16.94	0.603	0.078	-0.431
Interval 13	0.624	0.075	66.22	0.009	26.23	15.85	0.604	0.080	-0.476
Interval 14	0.631	0.088	50.23	0.013	18.71	10.92	0.603	0.090	-0.342
Interval 15	0.630	0.084	53.60	0.012	21.17	12.45	0.607	0.089	-0.448
Interval 16	0.627	0.096	38.75	0.016	16.08	9.59	0.602	0.103	-0.474
Interval 17	0.577	0.117	20.47	0.028	10.24	7.58	0.560	0.127	-0.692
Interval 18	0.568	0.120	20.52	0.028	9.71	7.42	0.552	0.136	-0.718
Interval 19	0.523	0.116	19.46	0.027	9.52	8.68	0.495	0.125	-0.493
Interval 20	0.452	0.101	20.99	0.022	10.98	13.31	0.401	0.077	0.078
Interval 21	0.409	0.095	19.94	0.021	11.18	16.13	0.354	0.060	0.325
Interval 22	0.379	0.080	24.66	0.015	14.41	23.52	0.333	0.046	0.385
Interval 23	0.353	0.073	26.54	0.013	15.85	29.01	0.311	0.036	0.456
Interval 24	0.328	0.056	38.36	0.009	24.22	49.65	0.298	0.033	0.287
Interval 25	0.305	0.044	53.52	0.006	35.62	81.20	0.282	0.028	0.210
Interval 26	0.298	0.034	78.93	0.004	54.47	128.55	0.283	0.029	-0.064
Interval 27	0.289	0.026	126.85	0.002	88.33	217.15	0.278	0.021	-0.030
Interval 28	0.282	0.022	166.17	0.002	119.50	305.03	0.274	0.022	-0.322
Interval 29	0.278	0.021	179.09	0.002	127.93	332.63	0.269	0.018	-0.085
Interval 30	0.273	0.019	203.11	0.001	147.67	393.21	0.266	0.019	-0.247
Interval 31	0.272	0.022	166.83	0.002	120.11	321.95	0.262	0.018	-0.059
Interval 32	0.280	0.034	75.63	0.004	52.36	134.30	0.264	0.023	0.118
Interval 33	0.285	0.034	82.05	0.004	54.90	137.68	0.270	0.020	0.122
Interval 34	0.295	0.057	33.26	0.009	21.15	50.37	0.268	0.024	0.363

<b>Interval 35</b>	0.312	0.079	19.70	0.016	11.83	25.94	0.275	0.038	0.300
<b>Interval 36</b>	0.369	0.121	10.81	0.034	6.11	10.33	0.298	0.063	0.480
<b>Interval 37</b>	0.432	0.141	9.45	0.046	5.21	6.81	0.370	0.120	-0.080
<b>Interval 38</b>	0.487	0.128	13.88	0.035	7.25	7.63	0.445	0.127	-0.321
<b>Interval 39</b>	0.529	0.107	23.56	0.022	11.39	10.16	0.497	0.110	-0.390
<b>Interval 40</b>	0.570	0.096	34.02	0.017	15.10	11.40	0.548	0.105	-0.533
<b>Interval 41</b>	0.554	0.090	36.42	0.015	16.90	13.64	0.531	0.096	-0.471
<b>Interval 42</b>	0.583	0.095	37.29	0.016	15.56	11.11	0.551	0.094	-0.295
<b>Interval 43</b>	0.574	0.097	34.27	0.017	14.93	11.07	0.550	0.103	-0.482
<b>Interval 44</b>	0.572	0.083	47.13	0.012	20.40	15.26	0.549	0.086	-0.425
<b>Interval 45</b>	0.576	0.088	42.59	0.014	18.17	13.36	0.550	0.090	-0.396
<b>Interval 46</b>	0.570	0.088	41.98	0.014	18.11	13.66	0.546	0.092	-0.445

712

713



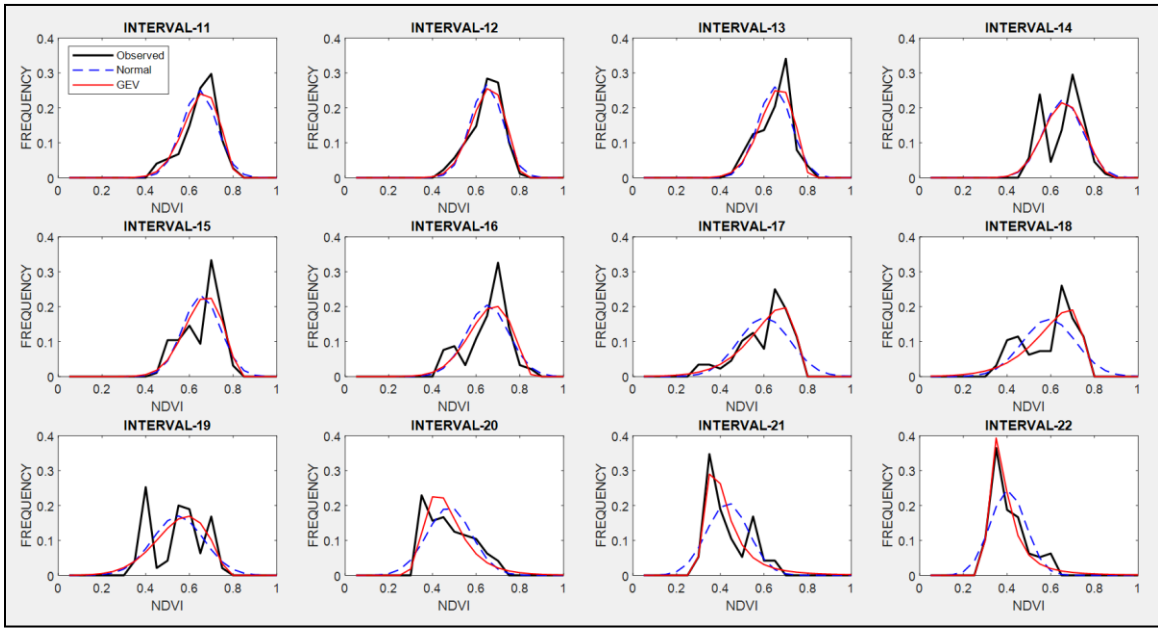
714

715

716

**Figure A1.** Observed NDVI, GEV and Normal probability density functions (PDF) from interval 45 to interval 10 (from 19 December to 21 March) representing winter.

717



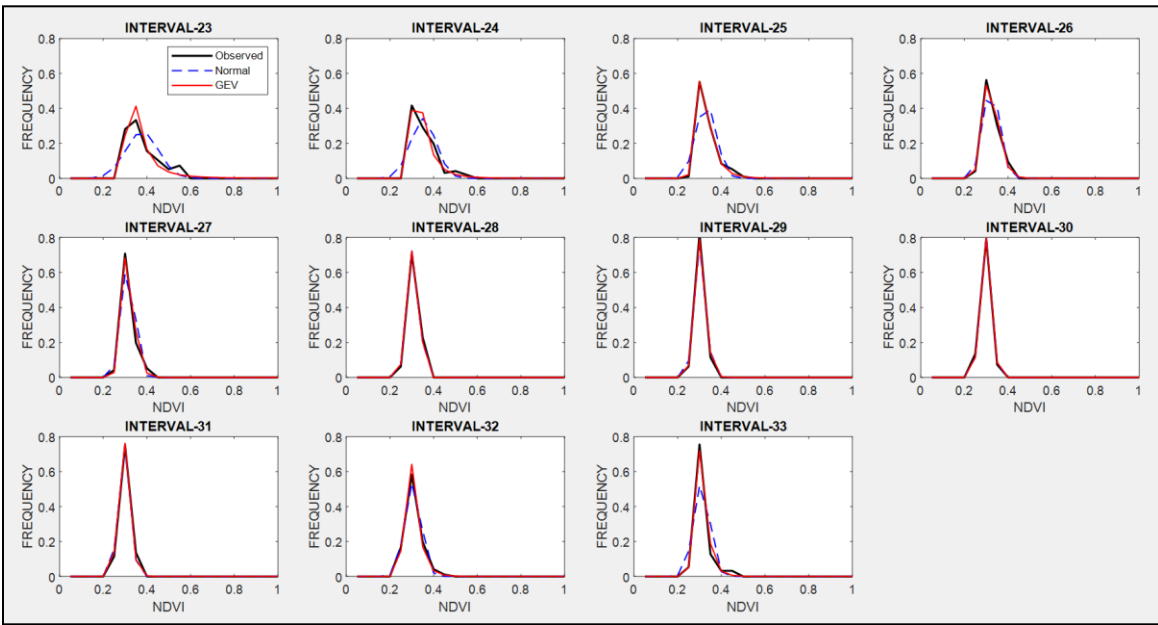
718

719

720

**Figure A2.** Observed NDVI, GEV and Normal probability density functions (PDF) from interval 11 to interval 22 (from 22 March to 25 June) representing spring.

721



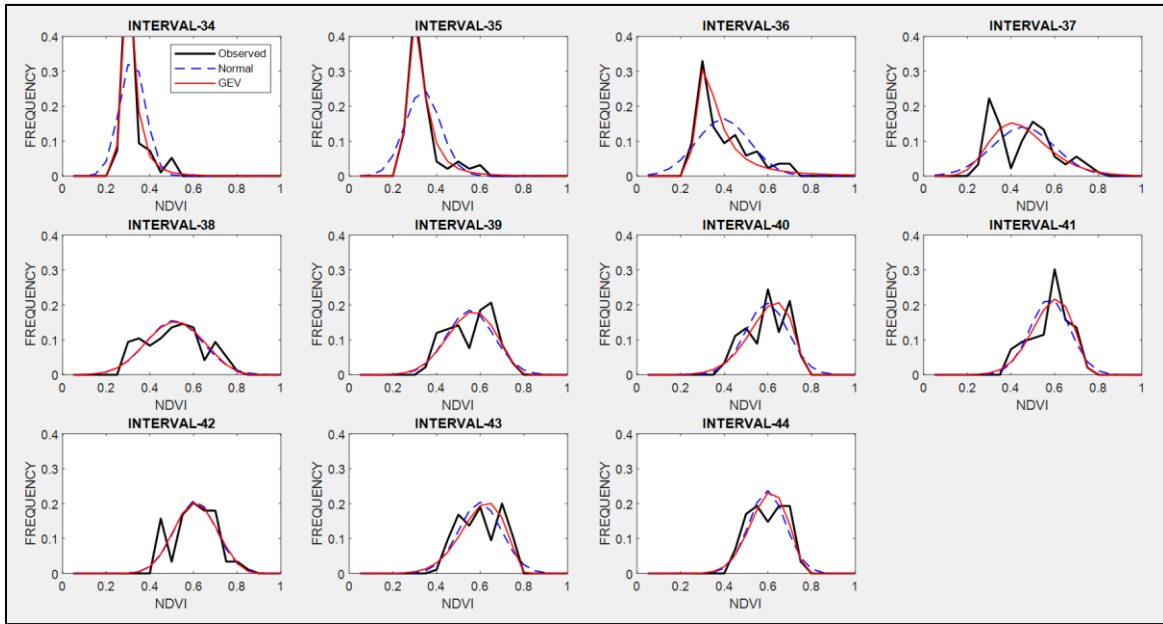
722

723

724

**Figure A3.** Observed NDVI, GEV and Normal probability density functions (PDFs) from interval 23 to interval 33 (from 26 June to 21 September) representing summer.

725



726

727

728

**Figure A4.** Observed NDVI, GEV and Normal PDFs from interval 34 to interval 44 (from 22 September to 18 December) representing autumn.

729

730 **References**

731

732 Agencia Estatal de Meteorología (AEMET). Available at: [www.aemet.es](http://www.aemet.es), 2017.

733 Al-Bakri, J. T., and Taylor, J. C.: Application of NOAA AVHRR for monitoring vegetation  
734 conditions and biomass in Jordan, *J. Arid Environ*, 54, 579–593, 2003.

735 Anyamba, A., and Tucker, C.J.: Historical perspective of AVHRR NDVI and vegetation  
736 drought monitoring. In: *Remote Sensing of Drought: Innovative Monit Approaches*, pp.  
737 23, 2012.

738 Bailey, S.: *The Impact of Cash Transfers on Food Consumption in Humanitarian Settings: A*  
739 *review of evidence, Study for the Canadian Foodgrains Bank, May 2013.*

740 Bayarjargal, Y., Karnieli, A., Bayasgalan, M., Khudulmur, S., Gandush, C., and Tucker, C.J.: A  
741 comparative study of NOAA-AVHRR derived drought indices using change vector  
742 analysis, *Remote Sens. Environ.* 105 (1), 9–22, 2006.

743 Boletín Oficial del Estado (BOE, 6638 - Orden AAA/1129/2013. Nº 145, III, p-46077, 2013.

744 Cochran, William G.: The Chi-square Test of Goodness of Fit, *Annals of Mathematical*  
745 *Statistics.* 23: 315–345, 1952.

746 Crimmins, M. A., and Crimmins T. M.: Monitoring plant phenology using digital repeat  
747 photography, *Environ. Manage*, 41, 949-958, 2008.

748 Dalezios, N. R., Blanta, A., Spyropoulos, N. V., and Tarquis A. M.: Risk identification of  
749 agricultural drought for sustainable Agroecosystems, *Nat. Hazards Earth Syst. Sci.*, 14,  
750 2435–2448, 2014.

751 Dalezios, N. R.: The Role of Remotely Sensed Vegetation Indices in Contemporary  
752 Agrometeorology. Invited paper in Honorary Special Volume in memory of late Prof. A.  
753 Flokas. Publisher: Hellenic Meteorological Association, 33-44, 2013.

754 De Leeuw, J., Vrieling, A., Shee, A., Atzberger, C., Hadgu, K. M., Biradar, C. M., Humphrey  
755 Keah, H., and Turvey, C.: The Potential and Uptake of Remote Sensing in Insurance: A  
756 Review, *Remote Sens.*, 6(11), 10888-10912, 2014.

757 Escribano Rodríguez, J. Agustín, Díaz-Ambrona, Carlos Gregorio H., and Tarquis Alfonso,  
758 Ana María: Selection of vegetation indices to estimate pasture production in Dehesas,  
759 *PASTOS*, 44(2), 6-18, 2014.

760 Fensholt, R., and Proud, S. R.: Evaluation of earth observation based global long term  
761 vegetation trends - comparing GIMMS and MODIS global NDVI time series, *Remote*  
762 *Sens. Environ.*, 119, 131–147, 2012.

763 Flynn E. S.: Using NDVI as a pasture management tool. Master Thesis, University of  
764 Kentucky, 2006.

765 Forkel, M., Carvalhais, N., Verbesselt, J., Mahecha, M.D., Neigh, C. S., and Reichstein, M.:  
766 Trend change detection in NDVI time series: effects of inter-annual variability and  
767 methodology, *Remote Sens.*, 5, pp, 2113–2144, 2013.



768 Fuller, D.O.: Trends in NDVI time series and their relation to rangeland and crop production  
769 in Senegal, 1987–1993, *Int. J. Remote Sens.*, 19, 2013–2018, 1998.

770 Gommès, R., and Kayitakire, F.: The challenges of index-based insurance for food security  
771 in developing countries. Proceedings, Technical Workshop, JRC, Ispra, 2-3 May 2012.  
772 Publisher: JRC-EC, p. 276, 2013.

773 Gouveia, C., Trigo, R. M., and Da Camara, C. C.: Drought and vegetation stress monitoring  
774 in Portugal using satellite data, *Nat. Hazards Earth Syst. Sci.*, 9, 185-195, 2009.

775 Goward, S. N., Tucker, C. J., and Dye, D.G.: North-American vegetation patterns observed  
776 with the NOAA-7 advanced very high-resolution radiometer. *Vegetation*, 64, 3–14,  
777 1985.

778 Graham, E. A., Yuen, E. M., Robertson, G. F., Kaiser, W. J., Hamilton, M. P., and Rundel, P.  
779 W.: Budburst and leaf area expansion measured with a novel mobile camera system  
780 and simple color thresholding, *Environ. Exp. Bot.*, 65, 238-244, 2009.

781 Hobbs, T. J.: The use of NOAA-AVHRR NDVI data to assess herbage production in the arid  
782 rangelands of central Australia, *Int. J. Remote Sens.*, 16, 1289–1302, 1995.

783 Holben, B. N.: Characteristics of maximum-value composite images from temporal AVHRR  
784 data, *Int. J. Remote Sens.*, 7, 1417–1434, 1986.

785 Kottek, M., Grieser, J., Beck, C., Rudolf, B., and Rubel, F.: World Map of the Köppen-Geiger  
786 climate classification updated, *Meteorologische Zeitschrift*, 15, 259-263, 2006.

787 Kundu, A., Dwivedi, S., and Dutta, D.: Monitoring the vegetation health over India during  
788 contrasting monsoon years using satellite remote sensing indices, *Arab J Geosci.*, 9,  
789 144, 2016.

790 Land Processes Distributed Active Archive Center (LP DAAC): Surface Reflectance 8-Day L3  
791 Global 500m. NASA and USGS. Available at:  
792 [https://lpdaac.usgs.gov/products/modis\\_products\\_Table/mod09a1](https://lpdaac.usgs.gov/products/modis_products_Table/mod09a1). 2014.

793 Larson, H. J.: *Introduction to Probability Theory and Statistical Inference* (3rd edition). New  
794 York, John Wiley and Sons, 1982.

795 Leblois, A.: Weather index-based insurance in a cash crop regulated sector: ex ante  
796 evaluation for cotton producers in Cameroon. Paper presented at the JRC/IRI  
797 workshop on The Challenges of Index-Based Insurance for Food Security in Developing  
798 Countries, Ispra, 2-3, May, 2012.

799 Lovejoy, S., Tarquis, A. M., Gaonac’h, H., and Schertzer, D.: Single and Multiscale remote  
800 sensing techniques, multifractals and MODIS derived vegetation and soil moisture.  
801 *Vadose Zone J.*, 7, 533-546, 2008.

802 Li, R., Tsunekawa, A., and Tsubo, M.: Index-based assessment of agricultural drought in a  
803 semi-arid region of Inner Mongolia, China, *J. Arid Land* 6 (1), 3–15, 2014.

804 Maples, J. G., Brorsen, B. W., and Biermachs, J. T.: The rainfall Index Annual Forage pilot  
805 program as a risk management tool for cool-season forage. *J. Agr. Appl Econ*, 48(1),  
806 29–51, 2016.

807 Martin-Sotoca, J. J., Saa-Requejo, A., Orondo J. B., and Tarquis, A. M.: Singularity maps  
808 applied to a vegetation index, *Bio. Eng.* 168, 42-53, 2018.

809 Motohka, T., Nasahara, K. N., Murakami, K., and Nagai, S.: Evaluation of sub-pixel cloud  
810 noises on MODIS daily spectral indices based on in situ measurements, *Remote Sens.*,  
811 3, 1644–1662, 2011.

812 Nanzad, L., Zhang, J., Tuvdendorj, B., Nabil, M., Zhang, S., and Bai, Y.: NDVI anomaly for  
813 drought monitoring and its correlation with climate factors over Mongolia from 2000  
814 to 2016, *Journal of Arid Environments* Volume 164, Pages 69-77, 2019.

815 Niemeyer, S.: New drought indices, First Int. Conf. on Drought Management: Scientific and  
816 Technological Innovations, Zaragoza, Spain. Joint Research Centre of the European  
817 Commission, Available online at  
818 <http://www.iamz.ciheam.org/medroplan/zaragoza2008/Sequia2008/Session3/S.Niemeyer.pdf>, 2008.  
819

820 Ortega-Farias, S., Ortega-Salazar, S., Poblete, T., Kilic, A., Allen, R., Poblete-Echeverría, C.,  
821 Ahumada-Orellana, L., Zuñiga, M., and Sepúlveda, D.: Estimation of Energy Balance  
822 Components over a Drip-Irrigated Olive Orchard Using Thermal and Multispectral  
823 Cameras Placed on a Helicopter-Based Unmanned Aerial Vehicle (UAV), *Remote Sens.*,  
824 8, 638, pp 18, 2016.

825 Park, S.: Cloud and cloud shadow effects on the MODIS vegetation index composites of the  
826 Korean Peninsula, *Int. J. Remote Sens.*, 34, 1234–1247, 2013.

827 Peters, A. J., E. A. Walter-Shea, L. Ji, A. Vina, M. Hayes, and M.D. Svoboda: Drought  
828 monitoring with NDVI-Based Standardized Vegetation Index, *Photogrammetric  
829 Engineering and Remote Sensing* 68:71–75, 2002.

830 Rao, K. N.: Index based Crop Insurance, *Agric. Agric. Sci. Proc.*, 1, 193–203, 2010.

831 Roumiguié, A., Sigel, G., Poilvé, H., Bouchard, B., Vrieling, A., and Jacquin, A.: Insuring  
832 forage through satellites: testing alternative indices against grassland production  
833 estimates for France, *Int. J. Remote Sens.*, 38, 1912-1939, 2017.

834 Roumiguié, A., Jacquin, A., Sigel, G., Poilvé, H., Lepoivre, B., and Hagolle, O.: Development  
835 of an index-based insurance product: validation of a forage production index derived  
836 from medium spatial resolution fCover time series, *GIScience Remote Sens.*, 52, 94-  
837 113, 2015.

838 Tackenberg, Oliver: A New Method for Non-destructive Measurement of Biomass, Growth  
839 Rates, Vertical Biomass Distribution and Dry Matter Content Based on Digital Image  
840 Analysis, *Annals of Botany*, 99(4), 777–783, 2007.

841 Turvey, C. G., and Mcaurin, M. K.: Applicability of the Normalized Difference Vegetation  
842 Index (NDVI) in Index-Based Crop Insurance Design, *Am. Meteorol. Soc.*, 4, 271-284,  
843 2012.

844 UNEP World Atlas of Desertification: Second Ed. United Nations Environment Programme,  
845 Nairobi, 1997.

846 USDA. U.S. Department of Agriculture, Federal Crop Insurance Corporation, Risk  
847 Management Agency: Rainfall Index Plan Annual Forage Crop Provisions. 16- RI-AF.  
848 <http://www.rma.usda.gov/policies/ri-vi/2015/16riaf.pdf> 2013 (Accessed March 1,  
849 2018).

850 Wei, W., Wu, W., Li, Z., Yang, P., and Qingbo Zhou, Q.: Selecting the Optimal NDVI Time-  
851 Series Reconstruction Technique for Crop Phenology Detection, *Intell. Autom. Soft. Co.*  
852 22, 237-247, 2016.

853

854

855

856